SUPPLEMENTAL MATERIAL

Supplemental material includes supplemental materials and methods, nine supplemental figures, and two supplementary tables.

Supplemental Materials and Methods

Reagents and antibodies Monoclonal anti-Flag M2 peroxidase antibody (A8592), monoclonal anti-HA peroxidase antibody (H6533), and anti-WIPI1 antibody (W2394) were from Sigma. Anti-CD3 antibody (ab5960), VeriBlot for IP detection reagent (HRP) (endogenous IP 2nd antibody, Ab131366), anti-phosphoserine antibody (ab9332), and anti-CD45R antibody (ab64100) were from Abcam. Anti-ATG16L antibody (PM040) and anti-LC3 antibody (PM036) were purchased from MBL. Anti-Beclin 2 antibody (NB110-60984) were obtained from Novus Biologicals. Anti-Mcl-1 antibody (sc-819) was from Santa Cruz. Anti-CXCR4 (PA3-305), anti-ATG9A antibody (for endogenous IP, PA5-85515), anti-ATG9A antibody (for western blot, PA1-16993), anti-STX7 antibody (PA5-76333), anti-STX8 antibody (PA5-48080), anti-RAB7A antibody (PA5-78238), anti-RAB8A antibody (PA5-79906), anti-RAB32A antibody (PA5-68304), anti-VAMP8 antibody (PA5-35300), and anti-Bcl7a (PA5-27123) were from Thermo Fisher. Anti-mouse CD3e-PerCP Cy5.5 (145-2C11, 45-0031-80), anti-mouse F4/80-PE (BM8, 12-4801-82), anti-mouse CD3e-pacific blue (eBio500A2, 48-0033-80), anti-mouse CD11b-pacific blue (M1/70, RM2828), anti-mouse CD3e-PE (145-2C11, 12-0031-81), and anti-mouse Gr-1-FITC (RB6-8C5, 11-5931-81) were obtained from Invitrogen. Anti-IL-21 (06-1074) was from EMD Millipore. Anti-Ki-67 antibody (12202S), anti-SQSTM1/p62 antibody (5114S), anti-Bcl-2 antibody (3498S), anti-p-STAT3 antibody (Tyr705) (9145L), anti-IL-1β antibody

(12242S), anti-MEKK3 antibody (5727S), anti-Stat3 antibody (9139S), anti-Erk5 antibody (3372S), anti-p-IKKα/ß antibody (2697S), anti-p-p44/42 MAPK antibody (Erk1/2) (9101S), anti-p44/42 MAPK antibody (9102S), anti-p-p38 MAPK antibody (9211S), anti-p38 MAPK antibody (9212S), anti-p-JNK antibody (9251S), anti-JNK antibody (9252S), anti-ULK1 antibody (8054S), anti-phospho-Stat3 (Tyr705) (9145L), anti-STX5 antibody (14151S), anti-STX6 antibody (2869S), anti-Beclin 1 (D40C5) antibody (3495S), and anti-WIPI2 antibody (8567S) were obtained from Cell Signaling Technology. InVivoMAb anti-mouse IL-6 (Clone MP5-20F3) was obtained from Bio X cell. Information regarding reagents, commercially available kits, and plasmids used in this study are listed in Supplementary Table 1.

Mouse breeding and experiments All animal experiments were performed in animal housing facilities under specific pathogen-free conditions at Houston Methodist Research Institute. All animal studies were performed according to the NIH guidelines for the use and care of live animals and approved by the Animal Care and Use Committee of the Houston Methodist Research Institute. Wild-type C57BL/6 mice and lysozyme-Cre (Lyz2-Cre) mice were obtained from Jackson Laboratory, *Becn2* KO mice were kindly provided by Dr. Beth Levine at University of Texas Southwestern Medical Center, Dallas. According to their publication (1), the heterozygous *Becn2* KO mice were backcrossed for more than 10 generations to C57BL/6J mice (Jackson Laboratories). We maintained both *Becn2* heterozygous and homozygous KO mice for breeding. *Becn2* KO mice were generated from both *Becn2* heterozygous and homozygous KO breeding pairs, WT mice were from *Becn2* heterozygous KO breeding pairs. The primer sequences for *Becn2* KO mice genotyping were listed in Supplementary Table 2. All mice were 6-12 weeks of age for experimental use, with the exception of mice for spontaneous tumor development. *Becn 2* KO mice were bred with *Map3k7*$^{\Delta M/\Delta M}$ mice (*Map3k7*$^{flox/flox}$ is provided by

M.D. Schneider, Baylor College of Medicine and bred with Lyz2-Cre to obtain *Map3k7*$^{\Delta M/\Delta M}$) or *Map3k3*$^{\Delta M/\Delta M}$ mice to generate *Map3k7*$^{\Delta M/\Delta M}$:*Becn2* KO and *Map3k3*$^{\Delta M/\Delta M}$:*Becn2* KO, respectively. *Becn1*$^{flox/flox}$ mice (from Knockout Mouse Project [KOMP] Repository) were bred with Lyz2-Cre mice (Jax Lab) to obtain *Becn1*$^{\Delta M/\Delta M}$ mice. For the LPS-induced endotoxic shock model, mice were i.p. injected with LPS (30 mg/kg body weight) and monitored for survival. Meanwhile, blood samples were collected to examine the proinflammatory cytokine levels. For macrophage depletion, clodronate-containing liposome was applied at 150 μL per mouse 16 h prior to LPS injection.

Cell culture HEK293T (CRL-3216) and THP-1 cells were purchased from ATCC. HEK293T cells were grown in DMEM supplemented with 10% fetal bovine serum (FBS) and 0.5% penicillin/streptomycin. THP-1 cells were grown in RPMI-1640 medium supplemented with 10% FBS, 0.5% penicillin/streptomycin, and 0.05 mM β-mercaptoethanol. BMDCs were prepared as previously described (2). Bone marrow was obtained from mouse femurs and tibias. Bone marrow progenitor cells were cultured in complete RPMI-1640 medium containing mouse granulocyte/macrophage colony-stimulating factor (GM-CSF, 20 ng/ml), mouse IL-4 (10 ng/ml) and β-Me (55 μM) for BMDC generation. Bone marrow progenitor cells were cultured in L929-cell conditioned medium for 5-6 days to obtain BMDMs. Peritoneal neutrophils were obtained from the peritoneal cavity by i.p. injection of 3 ml 4% (v/v) thioglycollate for 3 h, followed by peritoneal lavage with cold RPMI media/2% FBS. Cells were stained with anti-Gr-1-PE antibody (eBioscience) and purified using PE-positive selection magnetic beads (Stem Cell Technologies). For inflammasome activation studies, BMDCs or BMDMs were primed for 3 h with LPS (100 ng/ml), followed by treatment with ATP (5 mM) for 1 h. T cells were isolated from spleen and lymph nodes of 6- to 8-week-old mice and purified by untouched T cell selection kit (Thermo

Fisher). Splenic B cells were isolated from spleen and lymph nodes of 6- to 8-week-old mice by MagniSort Mouse B cell Enrichment Kit (Thermo Fisher).

Flow cytometry Cell suspensions were obtained from mouse tissues and stained for 20 min at 4°C in PBS containing 1% FCS and 10 mM EDTA with the indicated antibodies for cell surface staining. Flow cytometric analysis was performed with a BD FACSCalibur or BD FACSAria system (Becton Dickson). The acquired data were analyzed with FlowJo software.

CYTOF Spleen tissues isolated from WT and *Becn2* KO mice were mashed through 70-μm Nylon cell strainers and treated with RBC lysis buffer. Cells were washed twice with RPMI-1640 medium supplemented with 10% FBS, then stimulated with phorbol 12-myristate 13-acetate (PMA) for 4 h to activate the T cells. The single cell suspension was stained with metal-tag viability dye for 5 min and wash with cell staining buffer (Fluidigm), followed by staining of surface markers and intracellular markers separately. Cells were then stained with Cell ID Intercalator Ir (Fluidigm) at 4°C overnight. The next day, cells were washed and prepared for acquisition with Helios (Fluidigm). Cytobank (cytobank.org) was used for data analysis and generation of viSNE maps. Briefly, we analyzed ungated live cell populations for an equal number of events per sample after normalization, followed by gating on $CD45^+$ cell population. Lymphocyte populations were clustered in each viSNE map by CD4, CD8α, CD3ε, CD19, B220, IFN-γ, IL-4, IL-17A, Foxp3, CD10, CD23, CD21, and GL7 markers to display the lymphocyte subpopulations with different colors. The ratio of different cell populations within $CD45^+$ cells was quantified by Cytobank and plotted with Prism. The viSNE plots are shown as two-dimensional scatter plots with the x- and y-axes identified by tSNE1 and tSNE2.

Immunoprecipitation and immunoblot analyses To determine the interactions between endogenous Beclin 2 and the binding partners, 5 million cells were lysed using RIPA buffer and

incubate with 5 uL primary antibody against each partner protein respectively along with 30 uL Protein A/G beads, the immunoprecipitates were eluted with 2X SDS loading buffer. The secondary antibody (Veriblot for IP detection reagent HRP) that only recognized native IgG but not denatured IgG was applied for immunoblotting of proteins in immunoprecipitates. For immunoprecipitation of Flag-tagged proteins, cell lysates were incubated with anti-Flag beads (Sigma) at 4°C overnight. The beads were washed four times with RIPA lysis buffer, and immunoprecipitates were eluted with 2X SDS loading buffer. Immunoblotting was performed by loading the samples on SDS-PAGE gels, conducting electrophoresis, transferring the samples to PVDF membranes (Bio-Rad), and then incubating the membranes with the indicated antibodies. For all immunoblots, the LumiGLO Chemiluminescent Substrate System from KPL (Gaithersburg, MD) was used for protein detection.

ELISA Capture and detection antibodies for mouse TNF-α, IL-6, IL-1β, IL-10, IL-17, and IFN-γ (eBioscience) were used for the measurement of cytokines in cell supernatants and mouse sera according to the manufacturer's protocols.

Plasmids and cloning A complete open reading frame of human ATG proteins, RABs, and SNAREs, unless otherwise specified, were obtained from entry clone library (Human ORFeome library from Thermo Fisher or Baylor Ultimate ORF LITE) and subsequently subcloned into pcDNA3.1 or pEGFP-C2 vectors using PCR-based Gateway technology (Life Technologies). Plasmids encoding Flag-FIP200, RFP-ATG9A, and pUC57-APEX2 were obtained from Addgene (see Supplementary Table 1). Plasmids encoding MEKK3-APEX2 was cloned into pcDNA-3.1 vectors by homologous recombination using NEBuilder® HiFi DNA Assembly Cloning Kit.

Gene knockout by CRISPR technology in cells Gene knockout with CRISPR technology in THP1 cells and 293T cells were performed using the pLenti-Crispr-Cas9 v1 or v2 vectors (Addgene) containing gene-specific sgRNAs, followed by selection with Zeocin at 400 μg/ml for 5 days. Transduction of BMDMs using pLenti-Crispr-Cas9 system was started at day 2 after isolating progenitor cells from bone marrow. Lentiviruses produced by 293T cells were concentrated by centrifuging at 20,000 g for 2 h and resuspended in L929-cell conditioned medium for transduction. 16 h after transduction, the medium was replaced by the fresh L929-cell conditioned medium (for differentiation) and cells were recovered for 12 h, followed by selection with zeocin at 400 μg/ml for 4 days. On day 7, zeocin selection was withdrawal and LPS stimulation was started on day 7.5. The KO efficiency was confirmed by immunoblot analysis. The sgRNAs used for gene KO are listed in Supplementary Table 2.

Immunohistochemistry and immunofluorescence For immunohistochemistry, tissues were fixed overnight at room temperature in freshly prepared 4% paraformaldehyde and then embedded in paraffin. Formalin-fixed, paraffin-embedded tissues were sectioned into slices at a thickness of 5 μm then mounted onto glass slides. All sections used for immunohistochemistry were deparaffinized and hydrated using a graded ethanol series and deionized water. The tissues were incubated overnight at 4°C with primary antibodies, followed by labeling with HRP-conjugated or fluorescent probe-conjugated secondary antibodies (Alexa Fluor 488 anti-rat IgG or Alexa Fluor 555 anti-rabbit IgG). For immunofluorescence, tissues were mounted using ProLong® Gold Antifade Mountant with DAPI (P36941, Life Technology). Immunofluorescence using 293T cells was performed by transfecting cells with GFP-tagged MEKK3, GFP-Beclin 2, RFP-ATG9A, and/or Flag-Beclin 2 plasmids. To determine the transportation of GFP-MEKK3 into lysosome, cells were incubated with Lysotracker (Life Technology) and Hoechst 33342 at

24 h post-transfection. To determine the co-localization of GFP-MEKK3 and Flag-Beclin 2, cells were fixed by 4% paraformaldehyde and then incubated with anti-Flag antibody, followed by Alexa Fluor 633-conjugated anti-mouse IgG labeling. Microscopy was performed using a confocal microscope (Olympus, FV1000).

RNA extraction and real-time PCR Total RNA was extracted from cells or homogenized tissues using TRIzol reagent (Invitrogen) or Direct-zol™ RNA MiniPrep Plus w/ TRI Reagent® (ZYMO Research, R2071) following the manufacturer's protocol. cDNA was prepared using SuperScript IV Reverse Transcriptase (Thermo Fisher), and quantitative RT-PCR was performed using SYBR™ Green PCR Master Mix (Thermo Fisher) on a QuantStudio 6 Flex Real-time PCR System (Applied Biosystems). The RT-PCR primer sequences for each specific gene were listed in Supplementary Table 2.

RNA sequencing and analysis Total RNA was prepared from approximately 10 million cells or 20 μg of tissues by using TRIzol or the Direct-zol RNA MiniPrep Kit (Zymo Research). Each sample group contained two biological replicates. An RNA-seq library was prepared using Novogene's protocol. Briefly, mRNA was enriched using oligo(dT) beads and then fragmented randomly in fragmentation buffer. Next, cDNA was synthesized from these fragments using random hexamers and reverse transcriptase. After first-strand synthesis, a custom second-strand synthesis buffer (Illumina) was added along with dNTPs, RNase H and *Escherichia coli* polymerase I to generate the second strand via nick translation. The final cDNA library was sequenced using the Illumina HiSeq platform at Novogene. To compare gene expression levels under different conditions, a diagram of the distribution of fragments per kilobase of transcript sequence per million base pairs sequenced (FPKM) and a violin plot are used. DESeq, an R package based on a negative binomial distribution that models the number of reads from RNA-

seq experiments, was applied for the analysis of differentially expressed genes (DEGs). The threshold for DEGs was set as padj < 0.05 when using biological replicates in the experiments.

Enrichment of ATG9A$^+$ vesicles and autophagosomes 80% confluent WT, *STX5* KO, and *STX6* KO 293T cells were transfected with Flag-ATG9A and HA-Beclin 2, while *Becn2* KO 293T cells were transfected with Flag-ATG9A alone. Eight 15-cm dishes for each genotype were used for subsequent procedures. Half of the cells (4 dishes) were left untreated for immuno-isolation of Flag-ATG9A$^+$ vesicles, the other half were treated with CQ (10 μM, 4 h) to inhibit the fusion of autophagosomes with lysosomes to enrich autophagosomes prior to membrane fractionation. Membrane fractionation to enrich autophagosomes were performed as previously described (3). To isolate ATG9A-associated vesicles, cells were rinsed once in cold PBS at 24 h post-transfection, then scraped, spun down and resuspended in 2.7X of fractionation buffer (140 mM KCl, 1 mM EGTA, 5 mM $MgCl_2$, 50 mM Sucrose, 20 mM HEPES, pH 7.4, supplemented with protease inhibitor). Cells were mechanically broken by spraying 4-5 times through a 23G needle attached to a 1 ml syringe, then spun down at 2000 g for 10 min, yielding a post-nuclear supernatant (PNS) (4). Anti-Flag (100 μl, packed volume) was added to a 1.5 ml PNS aliquots and mixed by rotation at 4°C overnight. Beads with the associated membranes were washed with 1 ml immunoisolation buffer three times and membranes bound to the beads were eluted and lysed using RIPA buffer, followed by immunoblotting analysis. Immunoblotting of β-actin in whole cell lysates served as an input control. Autophagosome inputs were adjusted by similar LC3 amount for WT, *Becn2* KO, *STX5* KO, and *STX6* KO samples.

Transmission electron microscopy (TEM) and APEX2-enabled staining WT 293T cells with or without transfection of Flag-Beclin 2 were fixed in 2.5% (vol/vol) glutaraldehyde. The ultrathin sections (70-100 nm) of cell pellets were stained with lead citrate and uranyl acetate.

The samples were viewed under a JEOL JEM-1400 TEM. For EM imaging of MEKK3-APEX2, WT, *Becn2* KO, *STX5* KO or *STX6* KO cells were transfected and processed for staining following methods described previously (5, 6). Briefly, cells were fixed with Karnovsky's fixative, incubated in 3,3'-Diaminobenzidine (DAB) solution, post-fixed in osmium tetroxide, stained with uranyl acetate, dehydrated in a series of graded ethanol and embedded in epoxy resin. Sections of 100 nm thickness were cut using a Leica EM UC7 ultramicrotome. Electron micrographs were collected using a JEOL JEM-1230 TEM equipped with a Gatan CCD camera.

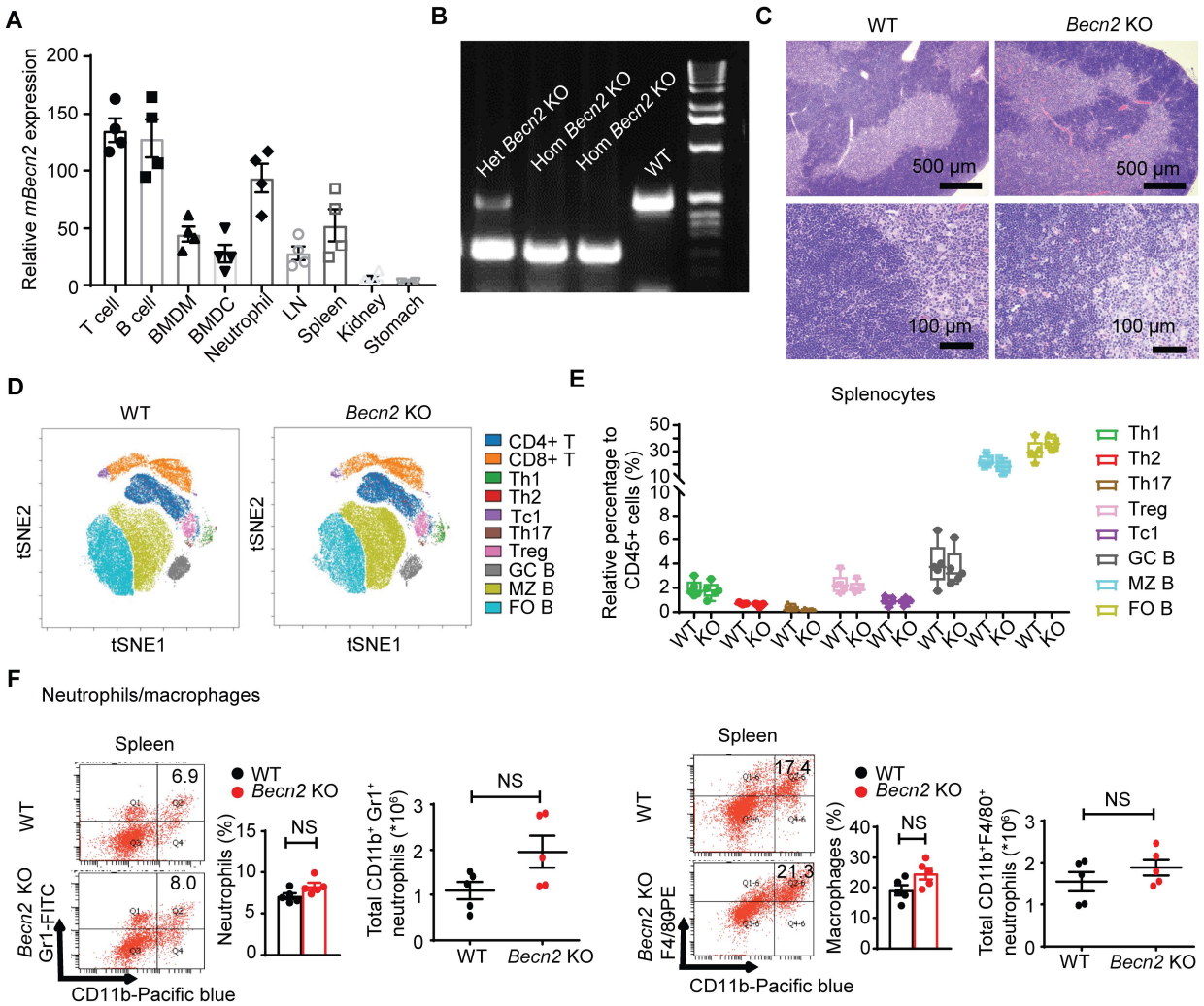

Supplemental Figure 1. Mouse genotyping and characterization for immune cell populations in *Becn2* KO mouse. (A) Real-time PCR for analysis of the mRNA levels of the mouse *Becn2* in indicated tissues or cell types (3 biological replicates for each group). (B) Genotyping for WT, heterozygous *Becn2* KO and homozygous *Becn2* KO mice. (C) H&E staining of thymus from WT and *Becn2* KO mice. (D, E) CYTOF analysis of T cell and B cell subsets in WT and *Becn2* KO splenocytes. viSNE map of representative WT and *Becn2* KO T cell and B cell subpopulations illustrated by color-coded cell populations that were clustered

together based on similarity in cell surface marker expression (D). (E) The percentage of lymphocyte subpopulations in total $CD45^+$ cells from spleen based on CYTOF analysis. (F) Flow cytometry and quantification analysis of $CD11b^+Gr1b^+$ neutrophil and $CD11b^+F4/80^+$ macrophage populations in the spleens from WT and *Becn2* KO mice. Statistical analysis is shown for at least three independent experiments and were calculated using Student's unpaired t-test.

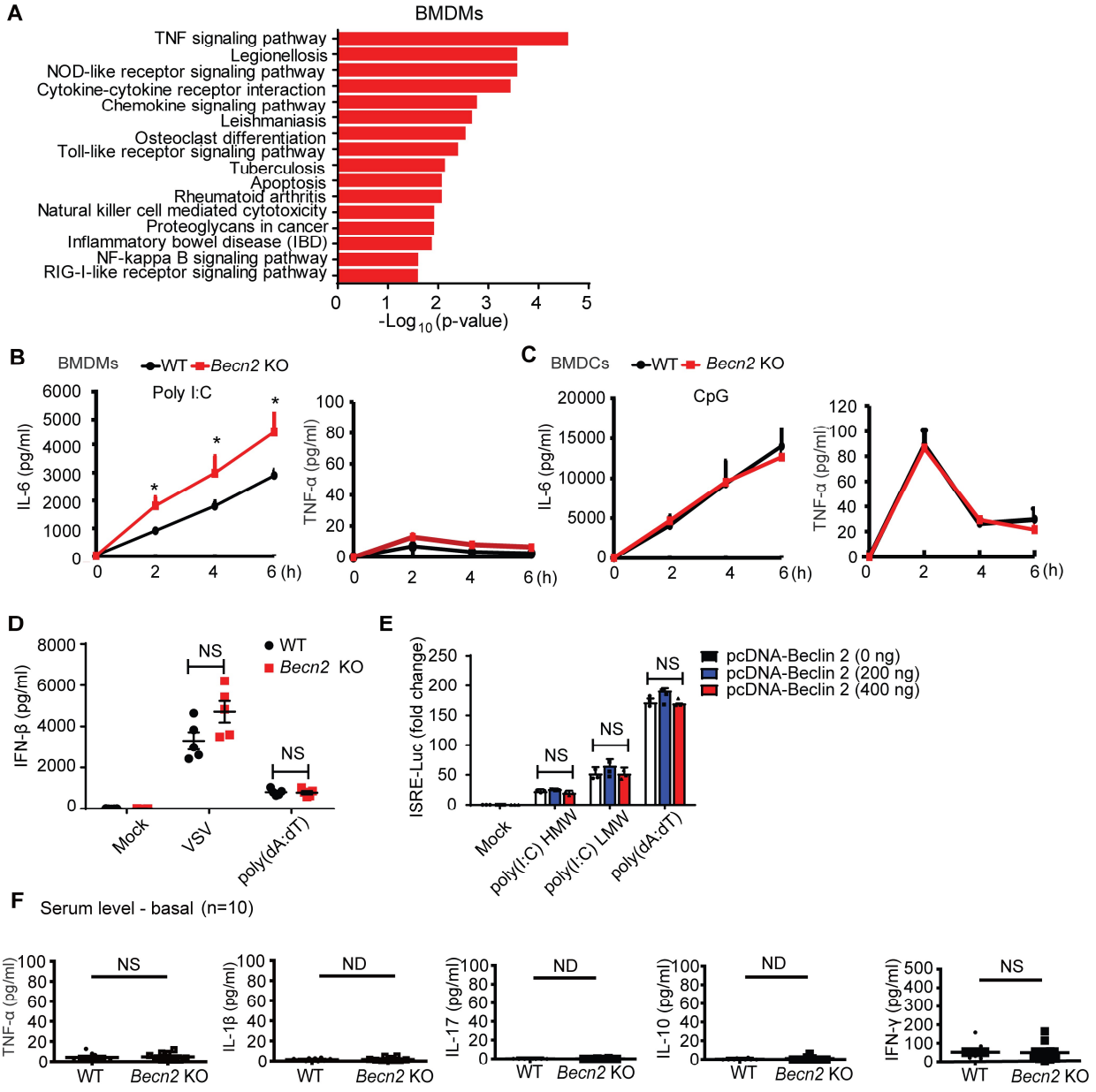

Supplemental Figure 2. Loss of Beclin 2 enhances pro-inflammatory cytokine production at mRNA levels. (A) The significantly enriched KEGG pathways in *Becn2* KO macrophages compared to WT macrophages after 3 h of LPS (100 ng/mL) stimulation. (B) Production of TNF-α and IL-6 from BMDMs transfected with poly I:C (2 μg/ml). (C) Production of TNF-α and

IL-6 by BMDCs treated with CpG (10 μg/ml). (D) IFN-β production of BMDMs at 24 h post VSV infection or poly(dA:dT) transfection. (E) 293T cells were co-transfected with increasing amounts of plasmids encoding Beclin 2 along with ISRE-Luc reporter, followed by stimulation with mock, poly(I:C) or poly(dA:dT). The luciferase expression in 293T cells was determined at 24 h post-stimulation. (F) TNF-α, IL-1β, IL-17, IFN-γ and IL-10 levels in 8- to 12-week old mice serum (n = 10 per group). Error bars represent mean ± s.e.m. Statistical differences between groups were calculated using Student's unpaired t-test (B, C, D, F) or 1-way ANOVA with Dunnett's multiple comparison test (E). Data are representative of at least three independent experiments (B-E). *$P < 0.05$. NS, no significance; ND, not detectable.

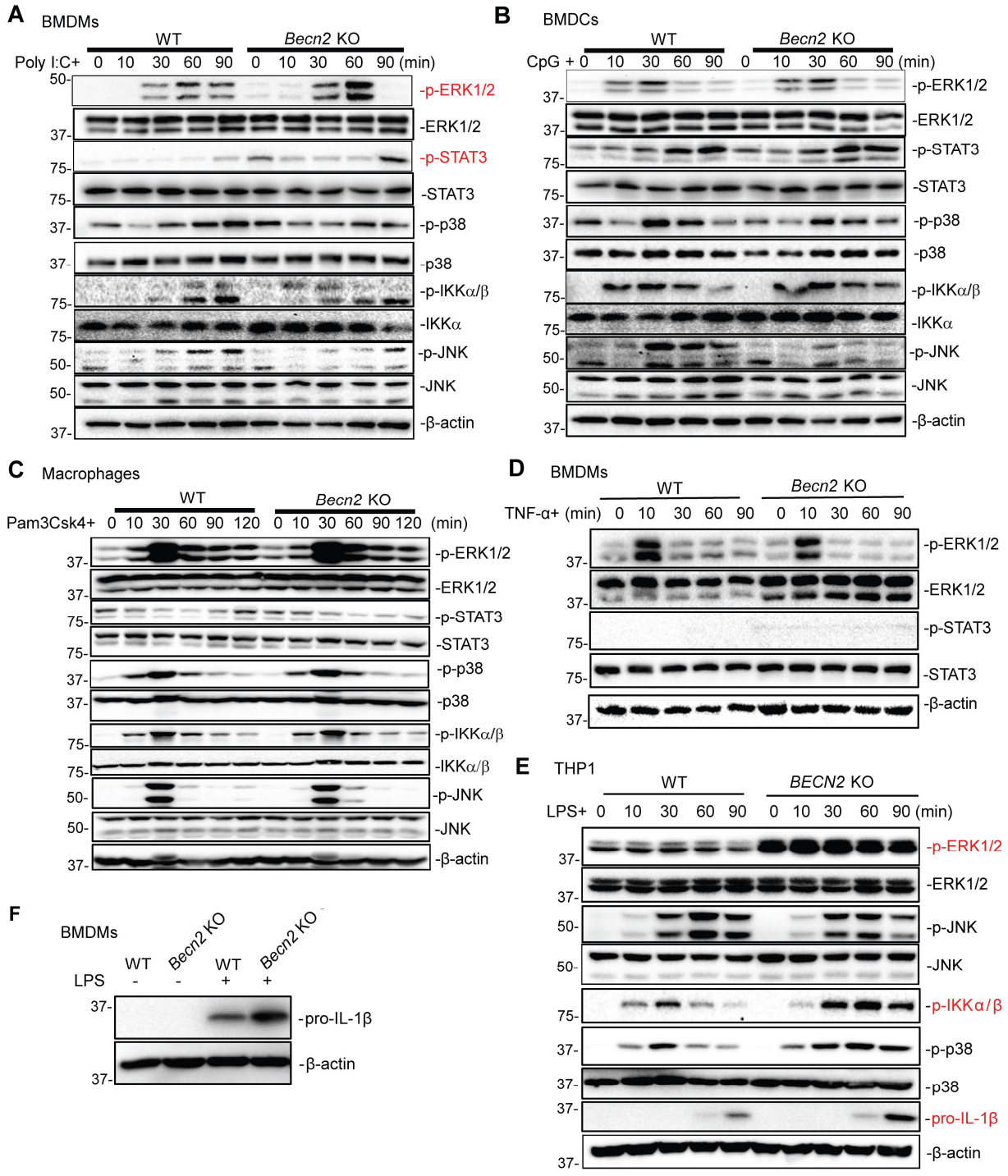

Supplemental Figure 3. Beclin 2 deficiency enhances ERK1/2 and STAT3 signaling in response to poly I:C but not CpG, Pam3CSK4, or TNF-α. (A) Immunoblot analysis of cell

lysates from WT or *Becn2* KO BMDMs transfected with poly I:C (2 μg/ml) for the indicated time points using indicated antibodies. (B) Immunoblot analysis of cell lysates from WT or *Becn2* KO BMDCs treated with CpG (10 μg/ml) for the indicated time points using the indicated antibodies. (C) Immunoblot analysis of cell lysates from WT or *Becn2* KO peritoneal macrophages treated with Pam3CSK4 (200 ng/ml) for the indicated time points using the indicated antibodies. (D) Immunoblot analysis of cell lysates from WT or *Becn2* KO BMDMs treated with TNF-α for the indicated time points using the indicated antibodies. (E) Immunoblot analysis of cell lysates from WT or *BECN2* KO THP-1 cells treated with LPS (100 ng/ml) for the indicated time points. (F) Immunoblot analysis of pro-IL-1β of cell lysates from WT or *Becn2* KO BMDMs treated with LPS (100 ng/ml) for 3 h. Data are representative of at least three independent experiments.

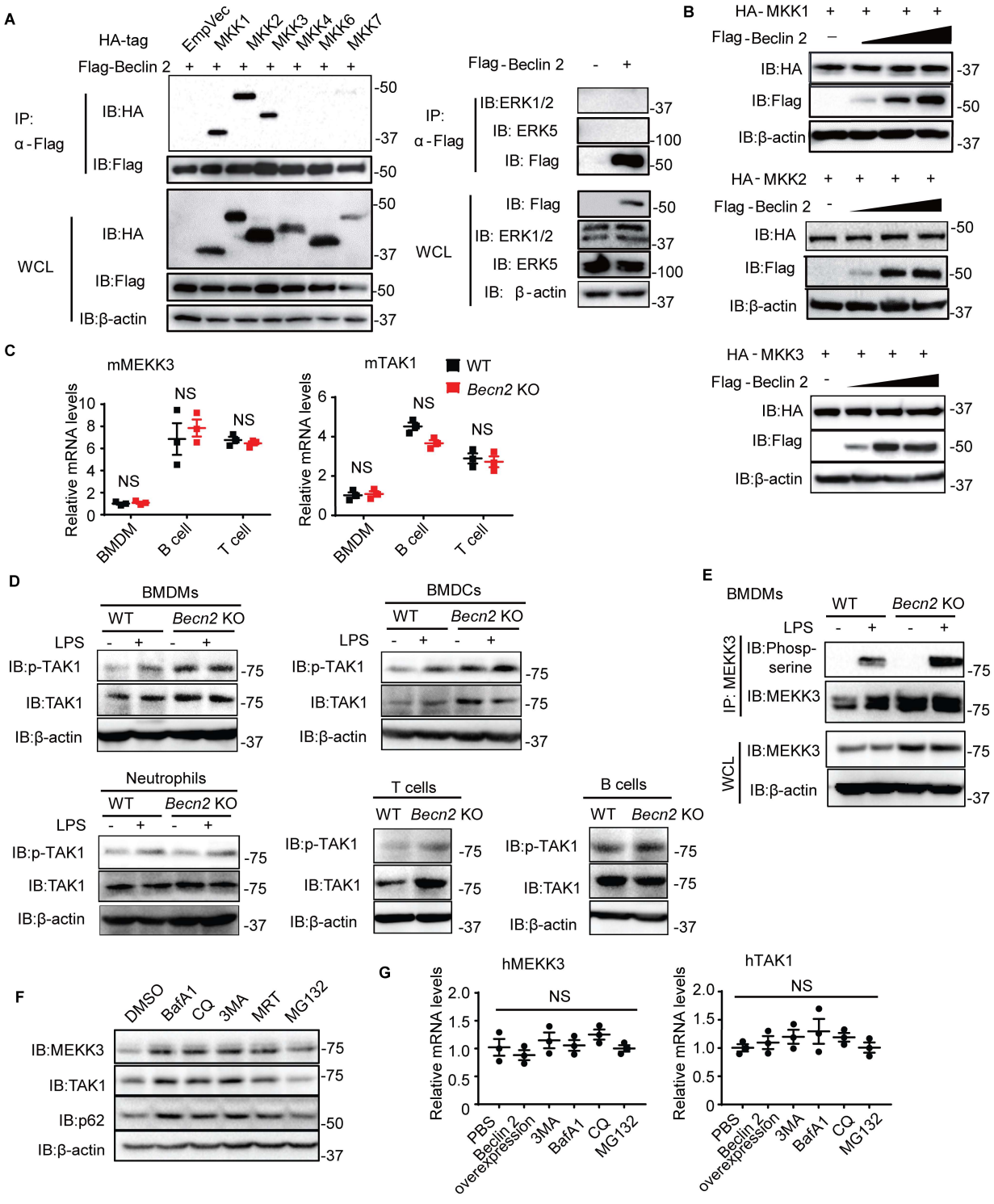
A
HA-tag
EmpVec
MKK1
MKK2
MKK3
MKK4
MKK6
MKK7
Flag-Beclin 2
IP: α-Flag
IB:HA
IB:Flag
WCL
IB:β-actin
IB:ERK1/2
IB: ERK5
IB: Flag
IB: β-actin
B
HA-MKK1
HA-MKK2
HA-MKK3
C
mMEKK3
mTAK1
WT
Becn2 KO
Relative mRNA levels
NS
BMDM
B cell
T cell
D
BMDMs
BMDCs
Neutrophils
T cells
B cells
LPS
IB:p-TAK1
IB:TAK1
E
IP: MEKK3
IB:Phosp-serine
IB:MEKK3
F
DMSO
BafA1
CQ
3MA
MRT
MG132
IB:p62
G
hMEKK3
hTAK1
PBS
Beclin 2 overexpression

Supplemental Figure 4. Beclin 2 targets TAK1 and MEKK3 for degradation. (A) 293T cells were co-transfected with the Flag-Beclin 2 plasmid alone or together with an HA-tagged plasmid were immunoprecipitated using anti-Flag beads, followed by immunoprecipitation with anti-Flag beads, then immunoblotting with the indicated antibodies. (B) Immunoblot analysis of 293T cells transfected with HA-MKK1 HA-MKK2 or HA-MKK3 alone, or together with increasing amount of Flag-Beclin 2 plasmid (100, 200 and 400 ng/10^6 cells). (C) Real-time PCR analysis of the mRNA levels of endogenous mouse TAK1 and MEKK3 in WT and *Becn2* KO BMDMs, splenic T cells and B cells. (D) Immunoblot analysis of p-TAK1 and TAK1 in cell lysates of WT and *Becn2* KO T cells, B cells, and macrophages, neutrophils and DCs before and after LPS (100 ng/ml, 30 min) treatment. (E) Cell lysates of BMDMs with or without LPS (100 ng/ml, 30 min) treatment were immunoprecipitated using anti-MEKK3 antibody, followed by immunoblotting with anti-phosphoserine antibody. (F) Immunoblot analysis of endogenous TAK1 and MEKK3 levels in 293T cells treated with Bafilomycin A (BafA, 500 nM), CQ (10 μM), 3MA (5 mM), MRT68921 (1 μM) or MG132 (10 μM) for 6-10 h. (G) Real-time PCR analysis of human TAK1 and MEKK3 mRNA levels in Beclin 2-overexpressed 293T cells or 293T cells treated with Bafilomycin A (BafA, 500 nM), CQ (10 μM), 3MA (5 mM), MRT68921 (1 μM) or MG132 (10 μM) for 6-10 h. Data are representative of three independent experiments. Statistical differences between groups were calculated using Student's unpaired t-test (C) or 1-way ANOVA (G). NS, no significance.

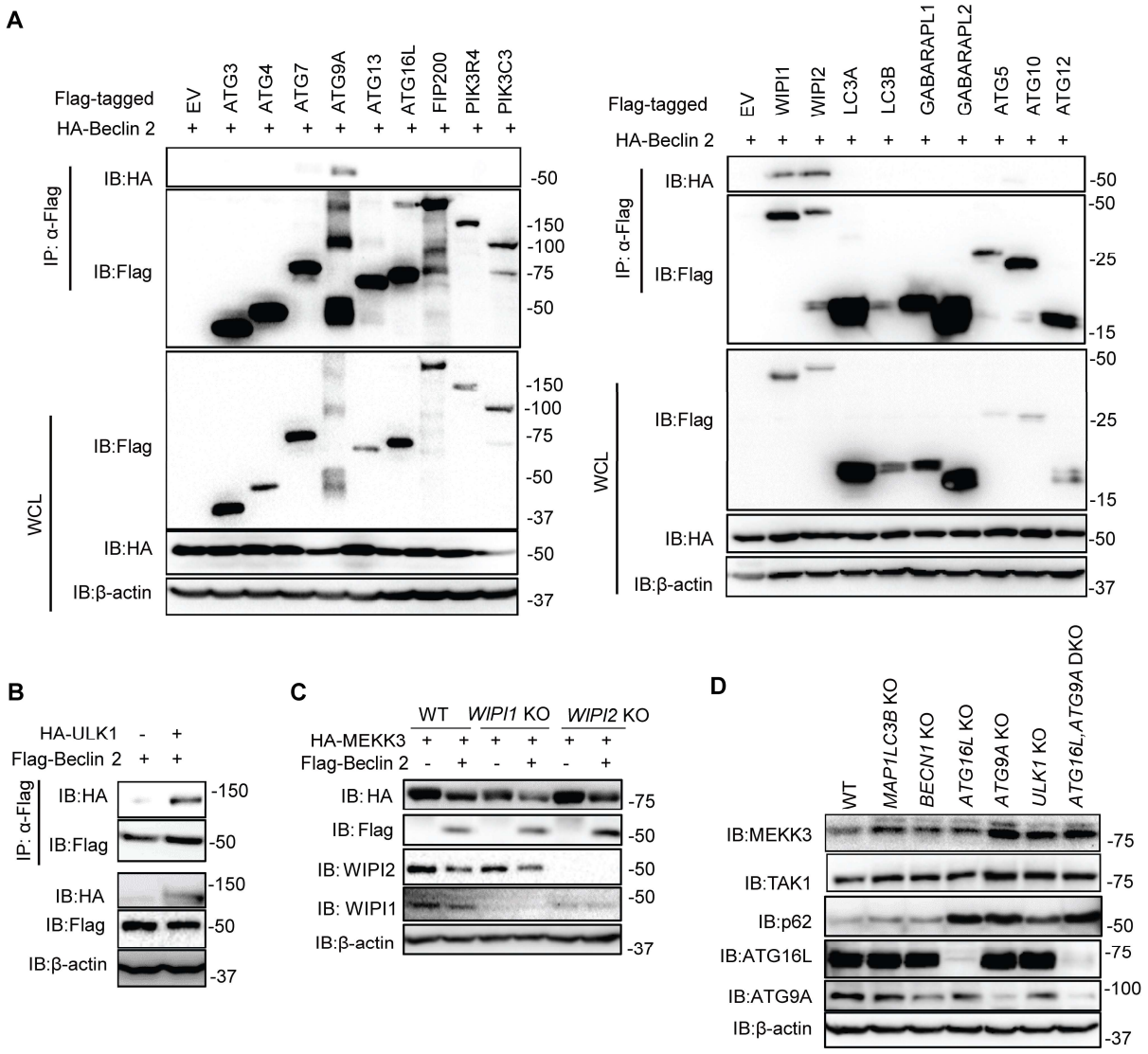

Supplemental Figure 5. Beclin 2 mediates the MEKK3 and TAK1 degradation through an ATG16L/LC3/Beclin 1-independent pathway. (A) 293T cells were co-transfected with HA-Beclin 2 and a Flag-tagged plasmid as indicated, followed by immunoprecipitation with anti-Flag beads, and then immunoblotting with the indicated antibodies. (B) 293T cells were co-transfected with Flag-Beclin 2 and HA-ULK1, 24 h post-transfection, cells were left in either complete medium or Earle's Balanced Salts medium for 4 h to induce starvation, followed by

immunoprecipitation with anti-Flag beads, and then immunoblotting with the indicated antibodies. (C) WT, *WIPI1* and *WIPI2*-sgRNA knockout 293T cells were co-transfected with HA-MEKK3 together with empty vector or Flag-Beclin 2 plasmid. Cell lysates were then immunoblotted with the indicated antibodies. (D) Immunoblot analysis of endogenous TAK1 and MEKK3 protein levels in the lysates of WT and *ATG* KO 293T cells using indicated antibodies. Data are representative of three independent experiments.

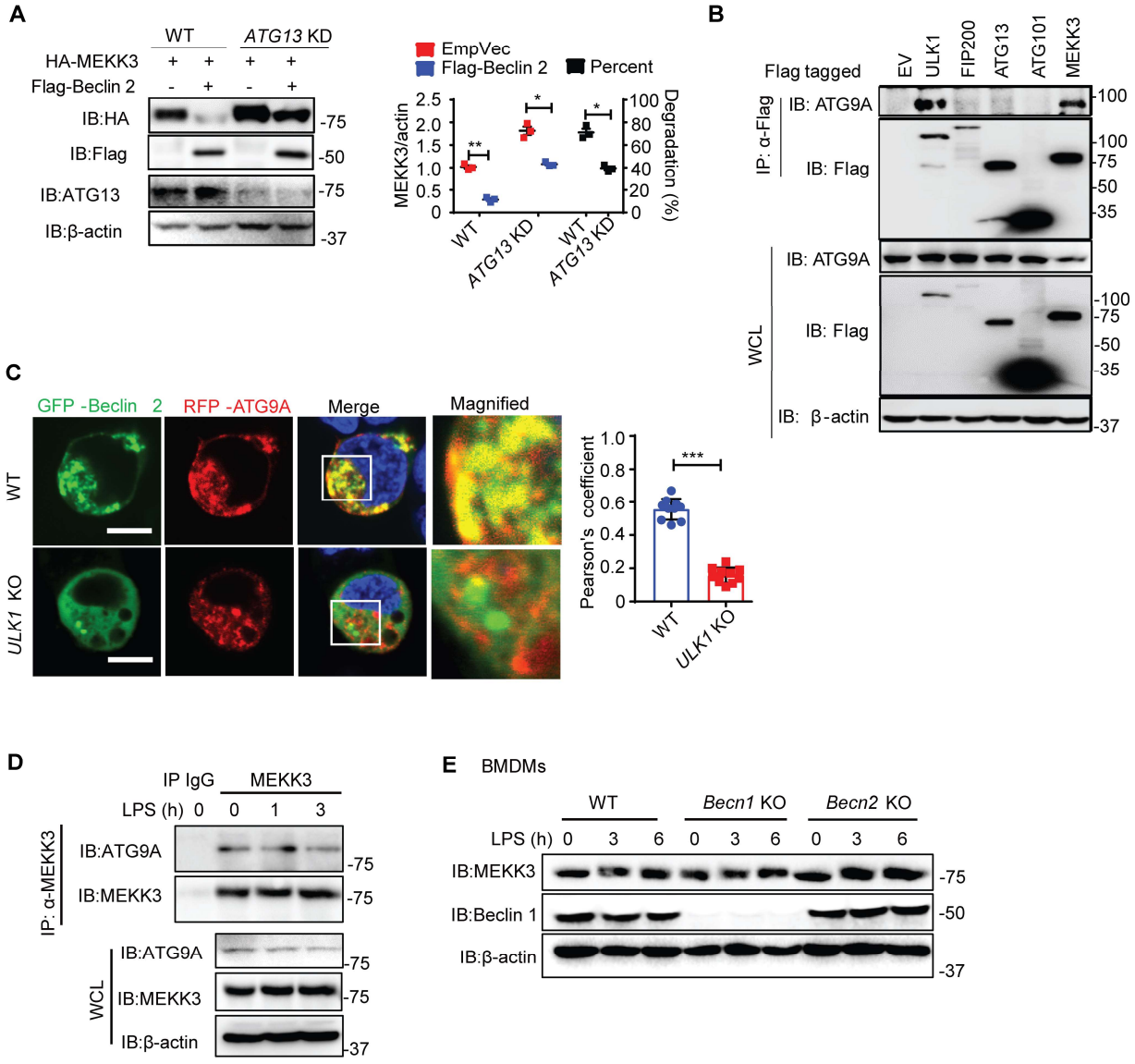

Supplemental Figure 6. Beclin 2 mediates the degradation of TAK1 and MEKK3 through an ATG9A- and ULK-dependent autophagic pathway. (A) WT and *ATG13* shRNA knockdown (KD) 293T cells were transfected with HA-MEKK3 alone or together with Flag-Beclin 2 plasmid, followed by immunoblotting with the indicated antibodies. Quantitative analysis of HA-TAK1 and HA-MEKK3 expression and degradation percentage in WT and *ATG13* knockdown cells based on band intensity of 3 independent experiments. (B) 293T cells were transfected with indicated Flag-tagged plasmid, followed by immunoprecipitation with

anti-Flag beads, and then immunoblotting with indicated antibodies. (C) Confocal images of WT and *ULK1* KO 293T cells co-transfected with GFP-Beclin 2 and RFP-ATG9A, then stained with Hoechst 33342 for nucleus imaging. Scale bar, 10 μm. Pearson's correlation coefficient for Beclin 2-ATG9A colocalization was analyzed using Image J Coloc 2. Graph represents mean ± s.d. (at least 30 cells were analyzed per condition). (D) BMDMs cells were left untreated or stimulated with LPS (100 ng/ml) for indicated time points, the cell lysates were then immunoprecipitated using MEKK3 antibodies, followed by immunoblotted with indicated antibodies. (E) Immunoblot analysis of endogenous MEKK3 protein levels in the lysates of WT, *Becn1* KO and *Becn2* KO BMDMs cells before and after LPS (100 ng/ml) stimulation. Data are representative of at least three independent experiments. Statistical differences between groups were calculated using Student's unpaired t-test (A, C). $*P < 0.05$; $**P < 0.01$; $***P < 0.001$.

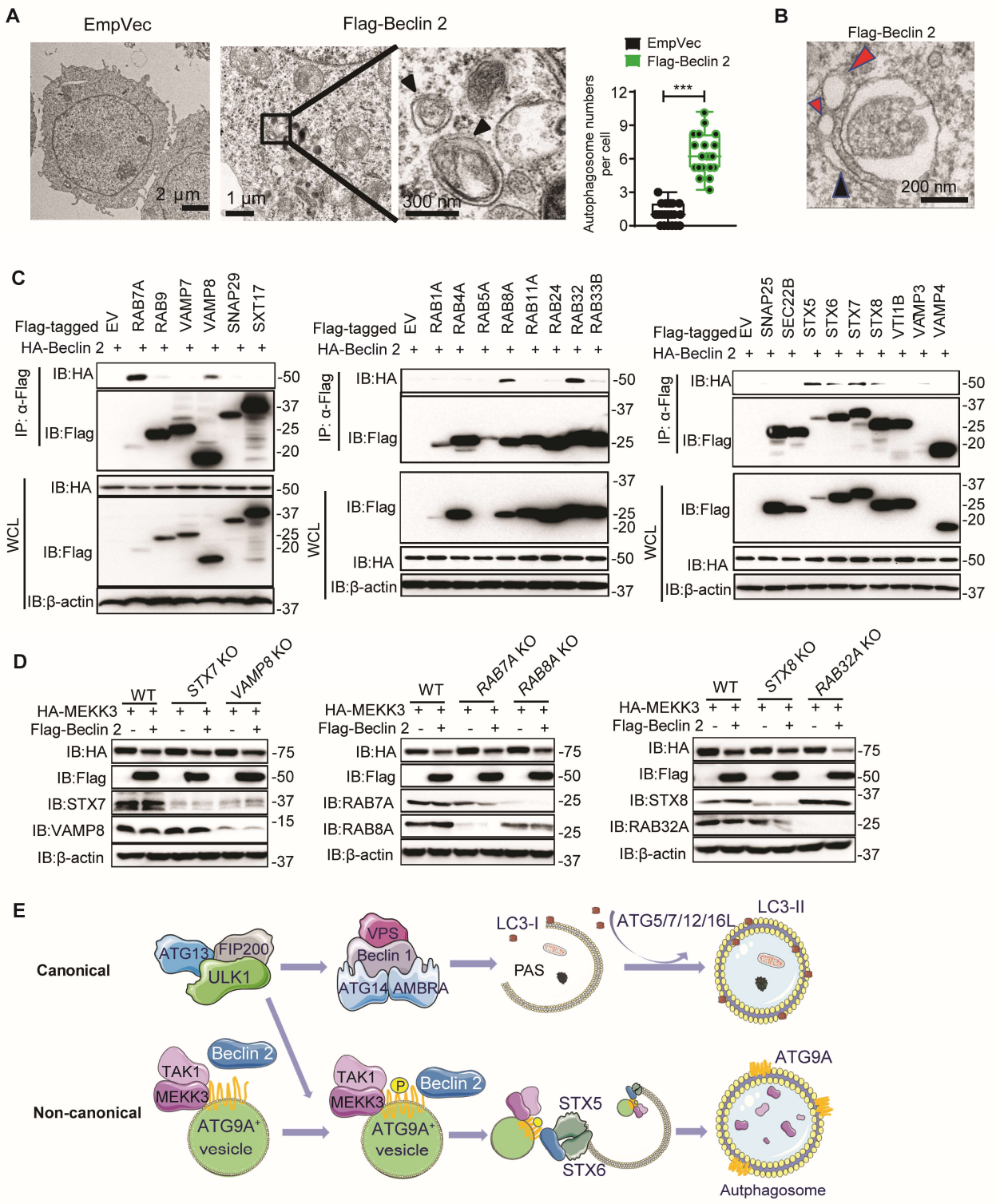
A
EmpVec
Flag-Beclin 2
2 μm
1 μm
300 nm
EmpVec
Flag-Beclin 2
Autophagosome numbers per cell
***
B
Flag-Beclin 2
200 nm
C
Flag-tagged EV RAB7A RAB9 VAMP7 VAMP8 SNAP29 SXT17
HA-Beclin 2
IP: α-Flag
IB:HA
IB:Flag
WCL
IB:β-actin
Flag-tagged EV RAB1A RAB4A RAB5A RAB8A RAB11A RAB24 RAB32 RAB33B
Flag-tagged EV SNAP25 SEC22B STX5 STX6 STX7 STX8 VTI1B VAMP3 VAMP4
D
WT STX7 KO VAMP8 KO
WT RAB7A KO RAB8A KO
WT STX8 KO RAB32A KO
HA-MEKK3
Flag-Beclin 2
IB:HA
IB:Flag
IB:STX7
IB:VAMP8
IB:RAB7A
IB:RAB8A
IB:STX8
IB:RAB32A
IB:β-actin
E
Canonical
ATG13
FIP200
ULK1
VPS
Beclin 1
ATG14
AMBRA
LC3-I
PAS
ATG5/7/12/16L
LC3-II
Non-canonical
Beclin 2
TAK1
MEKK3
ATG9A+ vesicle
P
STX5
STX6
ATG9A
Autphagosome

Supplemental Figure 7. Beclin 2 binds to STX5/6 to promote the fusion of ATG9A-vesicles with phagophores for MEKK3 degradation. (A) Transmission electron microscopy (TEM) images of WT and Flag-Beclin 2 transfected 293T cells. Black arrows indicate the double-membrane autophagosomal structures. The numbers of autophagosomes were counted. Graph represents mean ± s.d. (at least 30 cells were counted per condition). (B) EM image of vesicle fusion with pre-existing double-membrane structure in Flag-Beclin 2 transfected 293T cells. Black arrow indicates the pre-existing double-membrane structure; red arrows indicate the isolated membrane vesicles. (C) 293T cells were co-transfected with HA-Beclin 2 and a Flag-tagged plasmid as indicated, followed by immunoprecipitation with anti-Flag beads, and then immunoblotting with the indicated antibodies. (D) WT 293T cells or sgRNA-guided *RAB* or *SNARE* KO 293T cell were transfected with HA-MEKK3 alone or together with Flag-Beclin 2 plasmid, followed by immunoblotting with the indicated antibodies. (E) Schematic illustration of canonical autophagy pathway and Beclin 2-mediated non-canonical autophagic degradation of MEKK3/TAK1. PAS, phagophore assembly site. Statistical differences between groups were calculated using Student's unpaired t-test (A). ***$P < 0.001$.

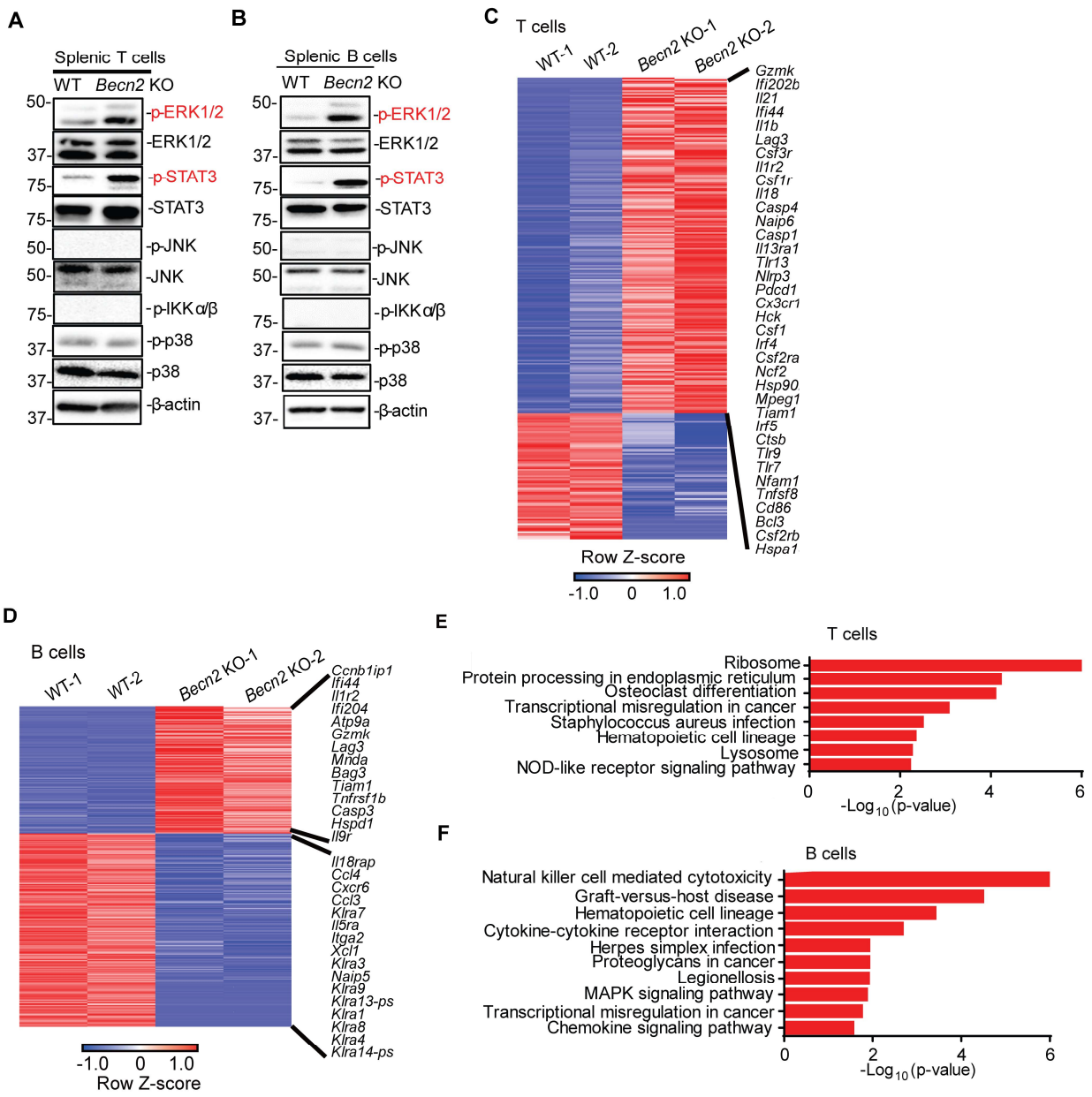

Supplemental Figure 8. Beclin 2 deficiency enhances ERK, STAT3 signaling in T cells and B cells and alters multiple immune signaling pathways. (A, B) Immunoblot analysis of cell lysates from WT or *Becn2* KO splenic T cells (A) and B cells (B) using the indicated antibodies. Data are representative of three independent experiments. (C, D) Heatmap of the DEGs in *Becn2* KO T cells (C) and B cells (D) compared with WT controls. The most significant DEGs involved in cytokine-cytokine receptor interaction and chemokine signaling pathways are listed on the

right side. (E, F) The significantly enriched KEGG pathways in *Becn2* KO splenic T cells (E) and B cells (F) compared to WT controls.

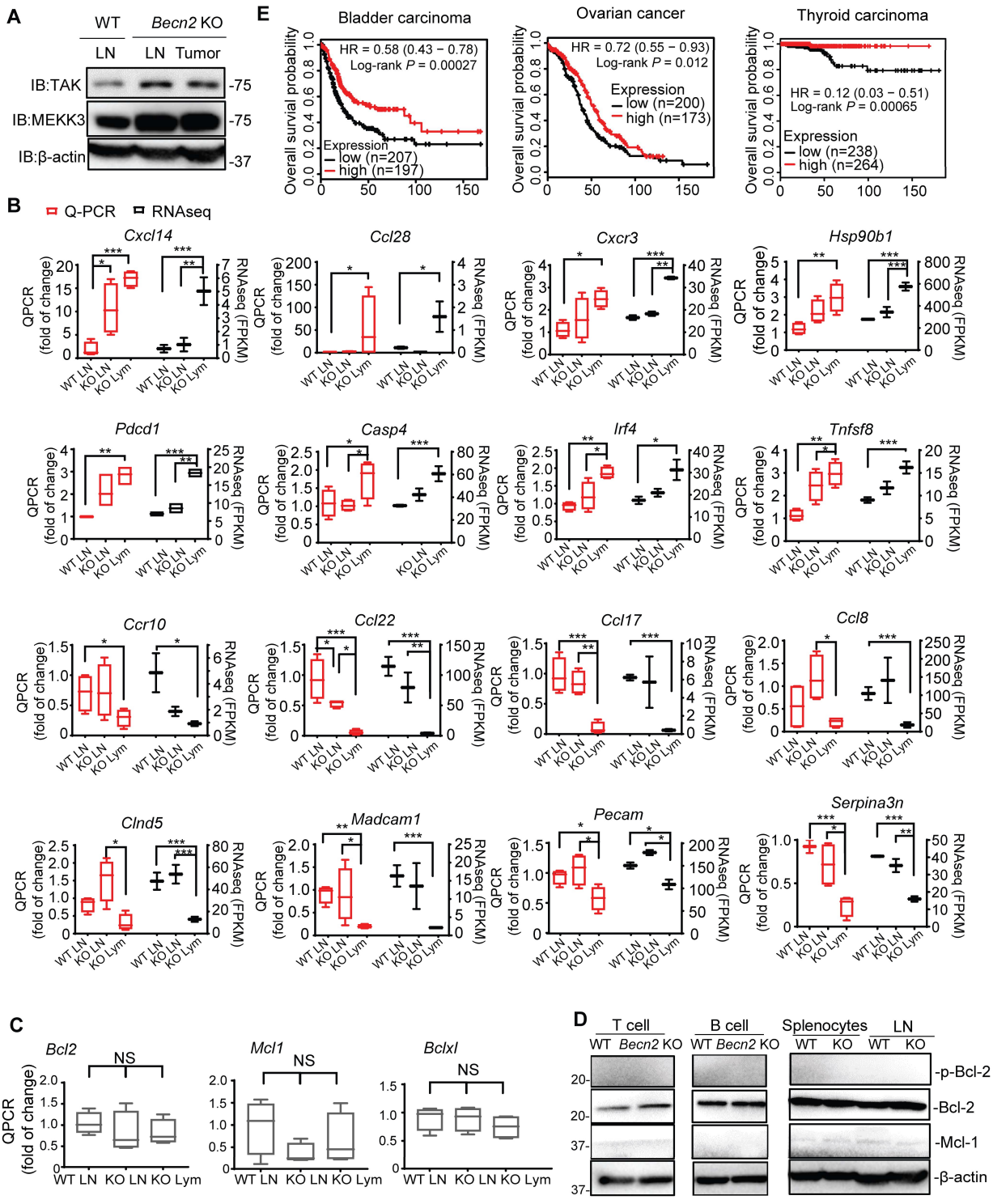
A
WT
Becn2 KO
LN
LN Tumor
IB:TAK
IB:MEKK3
IB:β-actin
-75
-75
-37
E
Bladder carcinoma
HR = 0.58 (0.43 − 0.78)
Log-rank P = 0.00027
Expression
low (n=207)
high (n=197)
Ovarian cancer
HR = 0.72 (0.55 − 0.93)
Log-rank P = 0.012
Expression
low (n=200)
high (n=173)
Thyroid carcinoma
HR = 0.12 (0.03 − 0.51)
Log-rank P = 0.00065
Expression
low (n=238)
high (n=264)
Overall survial probability
B
Q-PCR
RNAseq
Cxcl14
Ccl28
Cxcr3
Hsp90b1
Pdcd1
Casp4
Irf4
Tnfsf8
Ccr10
Ccl22
Ccl17
Ccl8
Clnd5
Madcam1
Pecam
Serpina3n
QPCR (fold of change)
RNAseq (FPKM)
WT LN
KO LN
KO Lym
C
Bcl2
Mcl1
Bclxl
NS
QPCR (fold of change)
WT LN
KO LN
KO Lym
D
T cell
B cell
Splenocytes
LN
WT
Becn2 KO
KO
-p-Bcl-2
-Bcl-2
-Mcl-1
-β-actin

Supplemental Figure 9. Spontaneous lymphoma development is associated with persistent activation of STAT3 signaling in *Becn2* KO mice. (A) Immunoblot analysis of TAK1 and MEKK3 expression in lymph nodes or lymphomas from WT and *Becn2* KO mice. (B) Real-time PCR for indicated gene mRNA levels in WT lymph nodes, *Becn2* KO lymph nodes, and *Becn2* KO lymphoma (4 biological replicates of each group) as compared to FPKM value of each gene from RNAseq analysis. (C) Real-time PCR analysis of the mRNA levels of *Bcl2*, *Bclxl* and *Mcl1* in WT lymph nodes, *Becn2* KO lymph nodes, and *Becn2* KO lymphoma (4 biological replicates for each group). Center line represents median in the whisker boxes, and upper and lower lines represent lowest to highest value. Statistical differences between groups were calculated using 1-way ANOVA with Tukey's multiple comparison test for Q-PCR data (B, C). **P* (Q-PCR) or *Padj* (RNAseq) < 0.05, ***P* (Q-PCR) or *Padj* (RNAseq) < 0.01, ****P* (Q-PCR) or *Padj* (RNAseq) < 0.001. NS, no significance. (D) Immunoblot analysis of for p-Bcl-2, Bcl-2, Bcl-xl and Mcl-1 protein levels in cell lysates of T cell, B cell, lymph nodes (LN), and splenocytes from WT and *Becn2* mice. (E) Kaplan-Meier plots depict the association between high *BECN2* expression and overall prolonged survival of patients with different cancer types. HR, hazard ratio. Log-rank test was used in the analysis.

Supplemental Tables

Supplementary Table 1. Reagents, kits, recombinant proteins, and plasmids.

Reagents, kits, and plasmids	Resources	Identifier
Lipopolysaccharides	Sigma	L3024
3-Methyladenine (3-MA)	Sigma	M9281
Bafilomycin A1 (autophagy inhibitor)	Sigma	B1793
Rapamycin (autophagy inducer)	Invivogen	tlrl-rap
MG132	Invivogen	tlrl-mg132
Pam3CSK4	Invivogen	tlrl-pms
Recombinant Mouse GM-CSF	Thermo Fisher Scientific	BMS325
Recombinant Mouse IL-4	Thermo Fisher Scientific	BMS338
ProLong® Gold Antifade Mountant with DAPI	Life Technology	P36941
DAB solution	Electron Microscopy Sciences	#13060
Dynabeads® Untouched™ Mouse T Cells Kit	Thermo Fisher Scientific	11413D
MagniSort Mouse B cell Enrichment Kit	Thermo Fisher Scientific	8804-6827-74
NEBuilder® HiFi DNA Assembly Kit	NEB	E2621
Direct-zol™ RNA MiniPrep Plus w/ TRI Reagent®	ZYMO Research	R2071
pMXs-puro-RFP-ATG9A	Addgene	#60609
p3xFLAG-CMV10-hFIP200	Addgene	#24300
pUC57-APEX2	Addgene	#40306
ProLong® Gold Antifade Mountant with DAPI	Life Technology	P36941
Dynabeads® Untouched™ Mouse T Cells Kit	Thermo Fisher Scientific	11413D
MagniSort Mouse B cell Enrichment Kit	Thermo Fisher Scientific	8804-6827-74
NEBuilder® HiFi DNA Assembly Kit	NEB	E2621
Direct-zol™ RNA MiniPrep Plus w/ TRI Reagent®	ZYMO Research	R2071

Supplementary Table 2. Oligo sequences for gene knockout, genotyping, and RT-PCR

Oligo sequences for gene knockout, genotyping, and RT-PCR
Primer for RT-PCR human (*BECN2*), forward ACTACAGTGCCTTGAAGCGG
Primer for RT-PCR human (*BECN2*), reverse CTCAAACGTGGCGGTGAAAC
Primer for RT-PCR mouse MEKK3, forward1 ATAAGGACACAGGTCACCCAA
Primer for RT -PCR mouse MEKK3, reverse1 TGCTCCACATCTTCGTATCTCA
Primer for RT-PCR mouse MEKK3, forward2 AGGTTCGGATCAAGCCTTCC
Primer for RT-PCR mouse MEKK3, reverse2 TGTCGCTCAGGTACATATCCC
Primer for RT-PCR mouse TAK1, forward1 CGGATGAGCCGTTACAGTATC
Primer for RT-PCR mouse TAK1, reverse1 ACTCCAAGCGTTTAATAGTGTCG
Primer for RT-PCR mouse TAK1, forward2 TGCCTTACTACACTGCTGCTC
Primer for RT-PCR mouse TAK1, reverse2 AAGCTGTACCAAAATCGCAGA
Primer for RT-PCR human MEKK3, forward1 GGCGAATTATAGCGTTCAGCC
Primer for RT-PCR human MEKK3, reverse1 GGGACAACAGCAATATCCTAAGG
Primer for RT-PCR human MEKK3, forward2 CAGGTGCGGATCAAGGCTT
Primer for RT-PCR human MEKK3, reverse2 CCGCTCAGGAACATAGCCAG
Primer for RT-PCR human TAK1, forward1 CCGGTGAGATGATCGAAGCC
Primer for RT-PCR human TAK1, reverse1 GCCGAAGCTCTACAATAAACGC
Primer for RT-PCR human TAK1, forward2 AAACCACCAAACTTACTGCTGG
Primer for RT-PCR human TAK1, reverse2 CGCGTTATCACTTCCCAAAGAA
Becn2 KO mouse genotyping, KO forward GTGAGTCGTATTAATTTCGATAAGCCAG
Becn2 KO mouse genotyping, WT forward CCCGGCTTAGACTTTTTTCTAAAGATG
Becn2 KO mouse genotyping, reverse GAGGTAAGCAGAGTAAAAGTGCAGAG
sgRNA for human *BECN2* knockout AAGAGCAGCGGCGGATCTCC
sgRNA for mouse ERK1 knockout CCACGTGCGCAAGACCAGAG
sgRNA for mouse ERK2 knockout GGTGCAGAACGTTAGCTGAA
sgRNA for human ATG16L1 knockout CAATTTAGTCCCGGACATGA
sgRNA for human *BECN1* knockout ATTTATTGAAACTCCTCGCC
sgRNA for human LC3B (*MAP1LC3B*) knockout TTCAAGCAGCGCCGCACCTT
sgRNA for human ATG9A knockout TCTGGAAACGGAGGATGCGG
sgRNA#1 for human ULK1 knockout TCTGCGGTTTCAGGTCGCGG
sgRNA#2 for human ULK1 knockout ATGATGGCGGCCACACTCTG
sgRNA#1 for human STX5 knockout TTAGACCCGTAGCGTTTCCG
sgRNA#2 for human STX5 knockout GCTTGGCAAATGTGTTGCTA
sgRNA#1 for human STX6 knockout TTGCCGAGTACTTGTAATGA
sgRNA#2 for human STX6 knockout CAAGTACTCGGCAAGTTGTC
sgRNA for human VAMP8 knockout TTATGACCCAGAATGTGGAG
sgRNA for human RAB7A knockout ACGGTTCCAGTCTCTCGGTG
sgRNA for human RAB8A knockout GTTGTCGAAGGACTTCTCGT
sgRNA for human RAB32 knockout GTCCCAGTTGAGGACCTTGA
sgRNA for human STX7 knockout GGATGTTAGAAGAGATCCTC
sgRNA for human STX7 knockout GAGTTACAAGATCATCCAAG

Supplementary references

1. He C, Wei Y, Sun K, Li B, Dong X, Zou Z, Liu Y, Kinch LN, Khan S, Sinha S, et al. Beclin 2 functions in autophagy, degradation of G protein-coupled receptors, and metabolism. *Cell.* 2013;154(5):1085-1099.
2. Inaba K, Inaba M, Romani N, Aya H, Deguchi M, Ikehara S, Muramatsu S, and Steinman RM. Generation of large numbers of dendritic cells from mouse bone marrow cultures supplemented with granulocyte/macrophage colony-stimulating factor. *J Exp Med.* 1992;176(6):1693-1702.
3. Stromhaug PE, Berg TO, Fengsrud M, and Seglen PO. Purification and characterization of autophagosomes from rat hepatocytes. *Biochem. J.* 1998;335 (Pt 2):217-224.
4. Zoncu R, Bar-Peled L, Efeyan A, Wang S, Sancak Y, and Sabatini DM. mTORC1 senses lysosomal amino acids through an inside-out mechanism that requires the vacuolar H(+)-ATPase. *Science.* 2011;334(6056):678-683.
5. Martell JD, Deerinck TJ, Lam SS, Ellisman MH, and Ting AY. Electron microscopy using the genetically encoded APEX2 tag in cultured mammalian cells. *Nat Protoc.* 2017;12(9):1792-1816.
6. Lam SS, Martell JD, Kamer KJ, Deerinck TJ, Ellisman MH, Mootha VK, and Ting AY. Directed evolution of APEX2 for electron microscopy and proximity labeling. *Nat Methods.* 2015;12(1):51-54.